

Supplementary information for

A facile, environmental-friendly synthesis of strong photo-emissive methylammonium lead bromide perovskite nanocrystals enabled by ionic liquids

Minh Tam Hoang^a, Ngoc Duy Pham^a, Yang Yang^a, Vincent Tiing Tiong^a, Chao Zhang^a, Ke Gui,^a Hong Chen^b, Jin Chang^b, Jianpu Wang^b, Dmitri Golberg^a, John Bell^{a,c} and Hongxia Wang^a

^a *School of Chemistry, Physics and Mechanical Engineering, Science and Engineering Faculty, Queensland University of Technology, Brisbane, QLD 4001, Australia*

^b *Key Laboratory of Flexible Electronics (KLOFE) & Institute of Advanced Materials (IAM), Nanjing Tech University (NanjingTech), 30 South Puzhu Road, Nanjing 211800, China*

^c *Division of Research and Innovation, University of Southern Queensland, PO Box 4393, Raceview, Qld 4305 Australia*

Experimental section

Synthesis of ionic liquids

All materials were purchased from Sigma-Aldrich and used as received unless otherwise stated. The ionic liquids were synthesized by acid-base reaction of methylamine (40 wt. % in H₂O) with either formic acid (≥95%), propionic acid (≥95%) or butyric acid (>99%) following previous report with a slight modification[1]. Specifically, 489.3 mmol of acids was added dropwise to methylamine (489.3 mmol) in an ice bath under magnetic stirring for 30 min. After all the carboxylate acid was added, the mixture was kept at 0°C under vigorous stirring for another 1 h. After that, the liquid material was collected through distillation using a rotary evaporator under low pressure at 60 °C.

Synthesis of perovskite nanocrystals

In a typical synthesis process, 50 mg of PbBr₂ was embedded in 2 ml of ionic liquid MAX (X=F, P, B) for a controlled reaction duration (1 min - 3 hrs). After that, the powder was collected through vacuum filtration. The collected powder was then pre-dried in a vacuum oven for 24 h at room temperature. The powder was then rinsed with 10 ml of Toluene, followed by centrifuging at 5000 rpm for 5 min to completely remove the residual ionic liquid.

Characterization

UV-visible absorbance of the samples was measured by a UV-visible spectrometer (Carry 60) and photoluminescence (PL) spectra of the samples were recorded with a Cary Eclipse Fluorescence Spectrophotometer. The high-resolution transmission electron microscopy (HRTEM) and selected area electron diffraction (SAED) images were captured by JEOL 2100 microscope operated at an accelerating voltage of 200 kV. Scanning electron microscopy (SEM) images of the samples were taken on a field emission SEM (FSEM, JOEL 7001 F) at an acceleration voltage of 5 kV or 10 kV. X-Ray Diffraction (XRD) patterns were recorded with a XRD equipment (Rigaku Smartlab) using monochromatic CuK α ($\lambda = 0.154$ nm) as a radiation source. Fourier transform infrared (FTIR) measurements were carried out using Bruker Alpha-P FTIR with ATR accessory. Proton nuclear magnetic resonance (NMR) measurement was conducted on a Bruker NMR Spectrometer, samples were diluted in D₆-DMSO. Time-resolved photoluminescence (TRPL) was measured by an Edinburgh fluorescence spectrometer at room temperature with a photoexcited wavelength of 474 nm and a pulse of 82.4 ps. Photoluminescence quantum efficiency (PLQY) measurements were performed using a home-made integrated setup including a laser, optical fibre, spectrometer and integrating sphere. Details on the measurement setup can be found in a previous report[2].

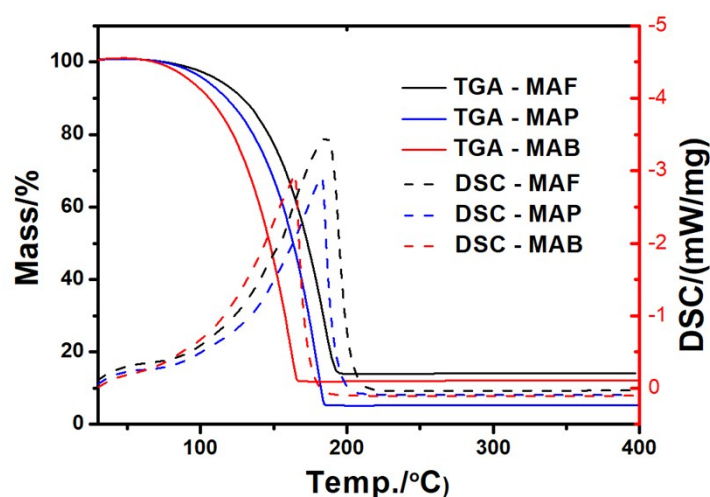


Figure S1: Thermal properties of the as-synthesized protonic Ionic liquid

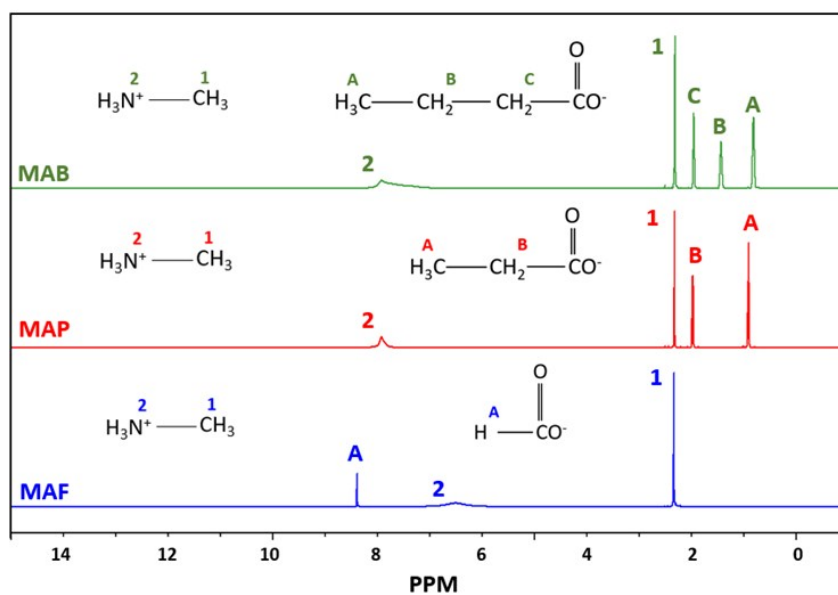


Figure S2: NMR spectra of as-synthesized MAF, MAP and MAB ILs. Inserted chemical structure of anion and cation with denoted chemical shift corresponding to NMR spectra.

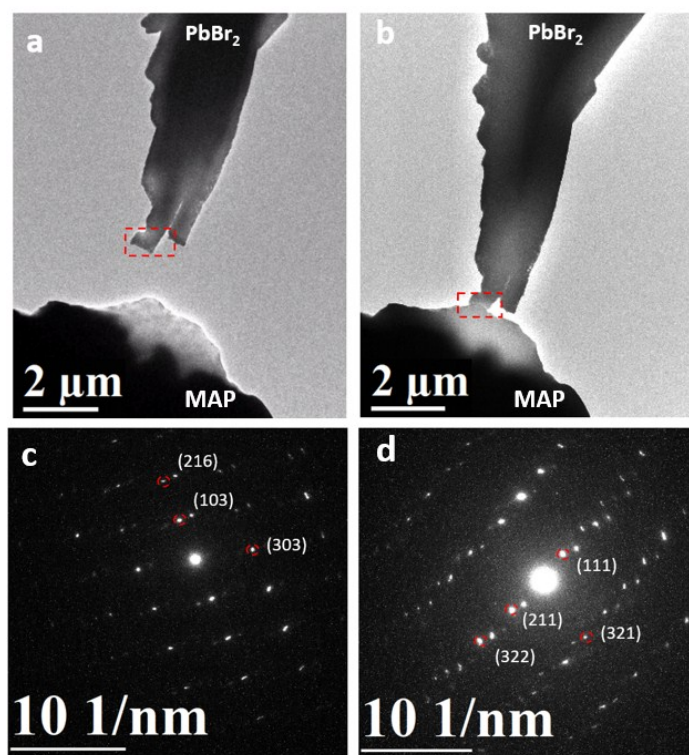


Figure S3: In-situ TEM measurement showing PbBr_2 (a) before and (b) after its contact with MAP ionic liquid; (c) SAD pattern from PbBr_2 before contact (collected from red rectangular area). The assigned diffraction pattern belongs to tetragonal PbBr_2 ; (d) SAD pattern after contacting with MAP with the appearance of new diffraction reflections assigned to the cubic MAPbBr_3 .

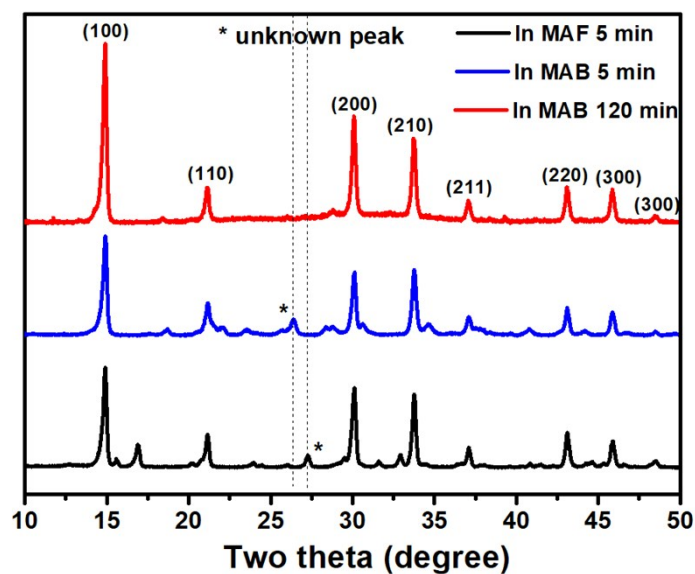


Figure S4: XRD spectrum of $\text{MAPbBr}_3(\text{MAB})$ and $\text{MAPbBr}_3(\text{MAF})$ formed at different reaction duration

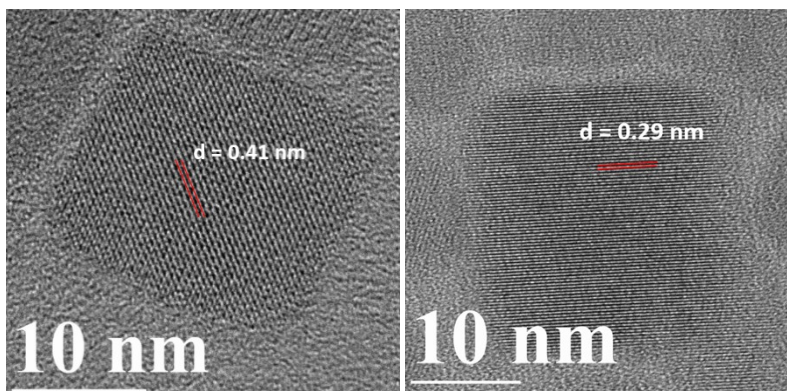


Figure S5: High resolution TEM image of $\text{MAPbBr}_3(\text{MAP})$ nanocube showing the lattice fringes of (110) and (200) planes

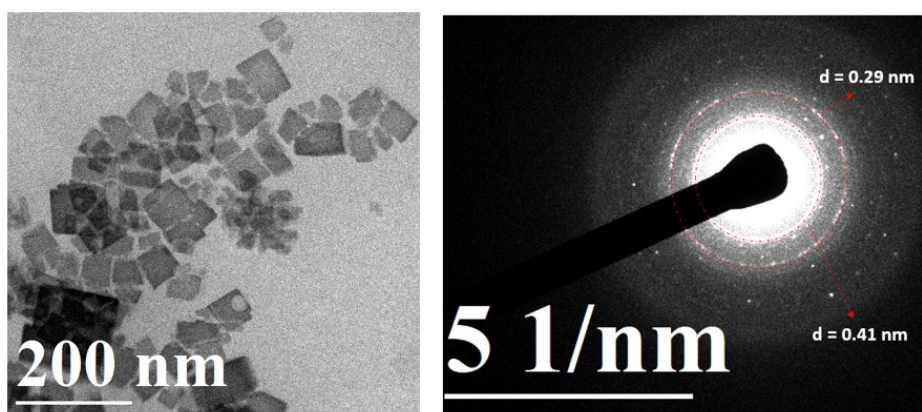


Figure S6: TEM images of $\text{MAPbBr}_3(\text{MAB})$ (left) and the corresponding selected area electron diffraction pattern (right).

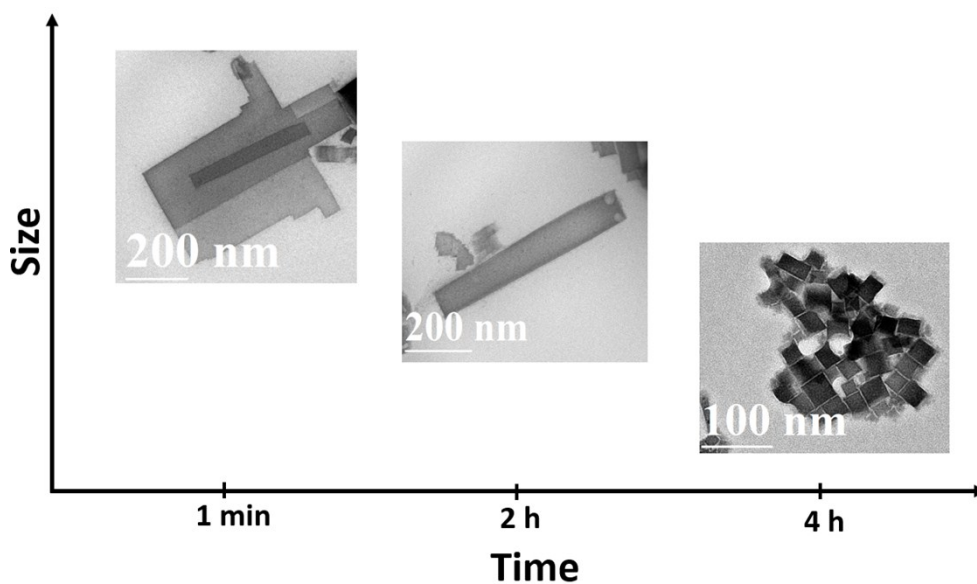


Figure S7: TEM images of $\text{MAPbBr}_3(\text{MAB})$ NCs collected at different stages of reaction time illustrating size and shape change of $\text{MAPbBr}_3(\text{MAB})$ NCs over reaction time.

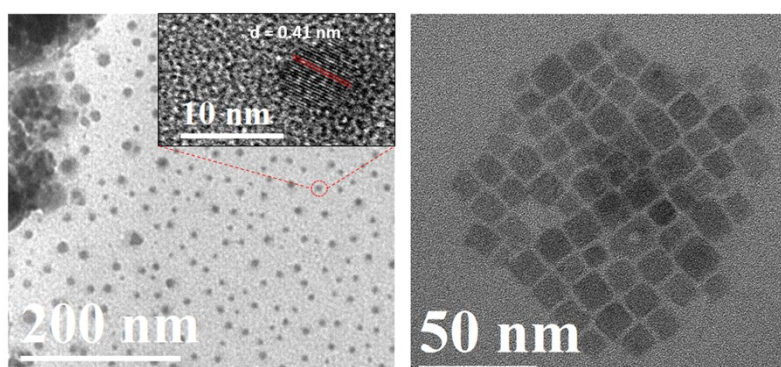


Figure S8: TEM images of $\text{MAPbBr}_3(\text{MAP})$ NCs collected after 1 min (left) and 2 hrs (right) of the reaction.

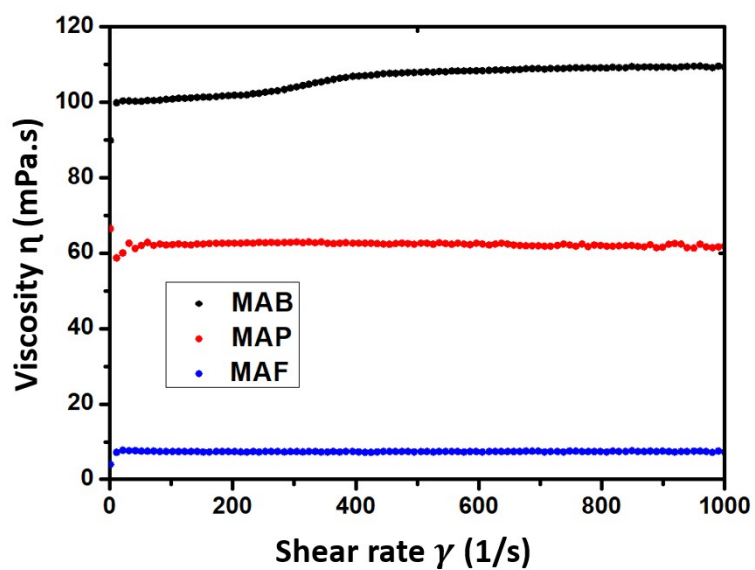


Figure S9: Comparison of viscosity of MAB, MAP and MAF ionic liquids.

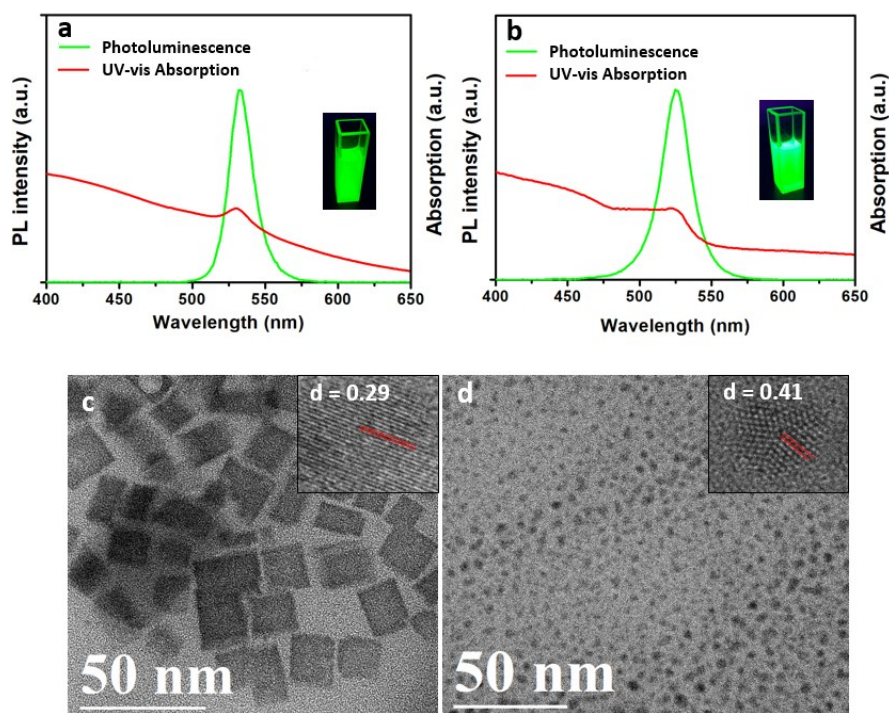


Figure S10: a) optical properties of MAPbBr₃(MAV); b) optical properties of MAPbBr₃(MABe) (Inserted picture of NCs solution under UV excitation); c) TEM images showing MAPbBr₃(MAV) NCs (inserted HR-TEM showing lattice fringe); d) TEM images showing MAPbBr₃(MABe) NCs (inserted HR-TEM showing lattice fringe)

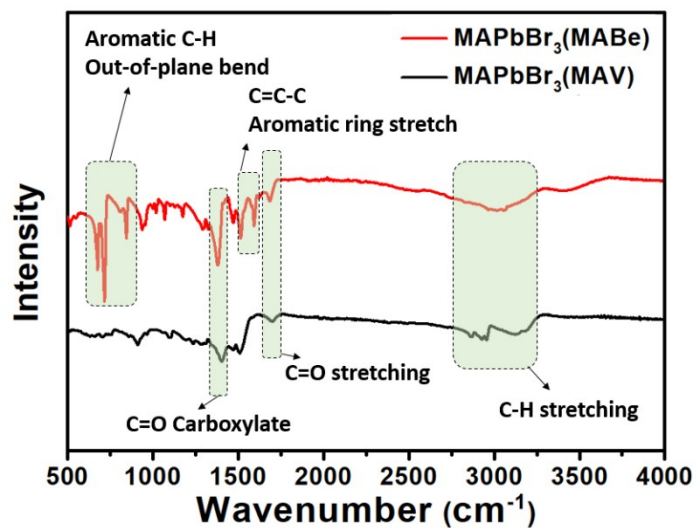


Figure S11: FTIR spectra of MAPbBr₃(MAV) and MAPbBr₃(MABe)

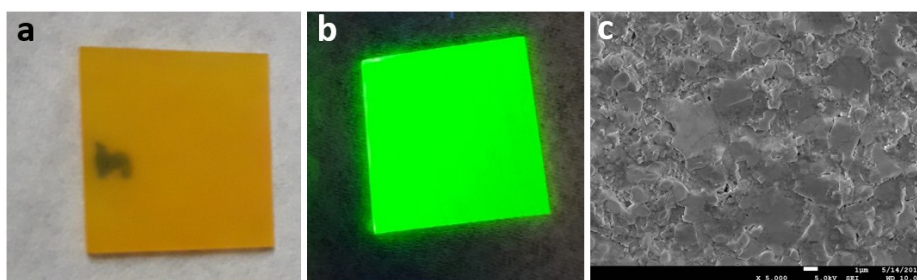


Figure S12: a) Doctor bladed thin film made from $\text{MAPbBr}_3(\text{MAB})$ perovskite ink; b) green emission of the thin film under UV-365 nm excitation and c) SEM image showing the morphology of the film.

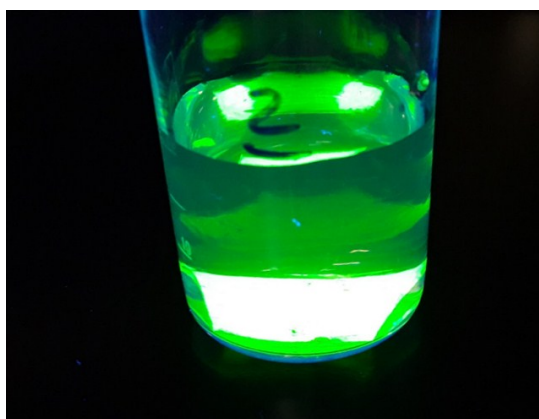


Figure S13: Optical image showing stability of the PeNCs thin film in water, where the PeNCs thin film still exhibits strong green emission under UV excitation.

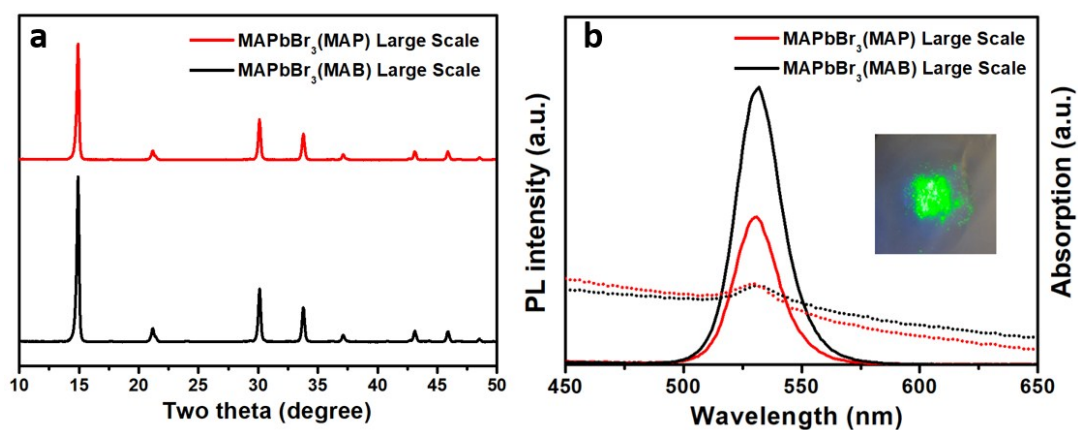


Figure S14: MAPbBr_3 NCs synthesis in 1g scale of PbBr_2 from MAP and MAB. a) XRD pattern and b) optical properties (inserted picture of final product $\text{MAPbBr}_3(\text{MAB})$ showing strong emission under 365nm UV excitation)

Table S1: Comparison of photoemission performance of NCs in this work with previous reports where different solvents were used.

Perovskite NCs	Solvent	PLQY thin film	PLQY solution	Ref
CH ₃ NH ₃ PbBr ₃	Ionic liquid (MAP, MAB)	50%	N/A	This work
CH ₃ NH ₃ PbBr ₃	DMF	23%	N/A	[3]
CH ₃ NH ₃ PbBr ₃	DMF & Octadecene	72%	83%	[4]
CH ₃ NH ₃ PbBr ₃	Octadecene	N/A	52% for platelet, 28% for cubes	[5]
CH ₃ NH ₃ PbI ₃	DMF, DMSO and THF	N/A	46%	[6]
CH ₃ NH ₃ PbBr ₃	HBr Acid	N/A	40%	[7]
CH ₃ NH ₃ PbI ₂ Br	Acetonitrile	30%	60-85%	[8]

Table S2: TR-PL Fitting data for the MAPbBr₃(MAB) and MAPbBr₃(MAP) doctor-bladed film.

Sample	τ_1 (ns)	A_1 (%)	τ_2 (ns)	A_2 (%)	χ^2	τ_{ave} (ns)
MAPbBr ₃ (MAB)	6.01	36.94	42.29	63.06	1.053	39.50
MAPbBr ₃ (MAP)	6.41	22.64	73.38	77.36	1.084	61.27

REFERENCES

- [1] S. Öz, J. Burschka, E. Jung, R. Bhattacharjee, T. Fischer, A. Mettenbörger, *et al.*, "Protic ionic liquid assisted solution processing of lead halide perovskites with water, alcohols and acetonitrile," *Nano Energy*, vol. 51, pp. 632-638, 2018.
- [2] J. C. de Mello, H. F. Wittmann, and R. H. Friend, "An improved experimental determination of external photoluminescence quantum efficiency," *Adv. Mater.*, vol. 9, pp. 230-232, 1997.
- [3] L. C. Schmidt, A. Pertegás, S. González-Carrero, O. Malinkiewicz, S. Agouram, G. Mínguez Espallargas, *et al.*, "Nontemplate synthesis of CH₃NH₃PbBr₃ perovskite nanoparticles," *J. Am. Chem. Soc.*, vol. 136, pp. 850-853, 2014.

- [4] S. Gonzalez-Carrero, R. E. Galian, and J. J. J. o. M. C. A. Pérez-Prieto, "Maximizing the emissive properties of CH₃NH₃PbBr₃ perovskite nanoparticles," vol. 3, pp. 9187-9193, 2015.
- [5] M. B. Teunis, M. A. Johnson, B. B. Muhoberac, S. Seifert, and R. J. C. o. M. Sardar, "Programmable Colloidal Approach to Hierarchical Structures of Methylammonium Lead Bromide Perovskite Nanocrystals with Bright Photoluminescent Properties," vol. 29, pp. 3526-3537, 2017.
- [6] F. Zhang, S. Huang, P. Wang, X. Chen, S. Zhao, Y. Dong, *et al.*, "Colloidal synthesis of air-stable CH₃NH₃PbI₃ quantum dots by gaining chemical insight into the solvent effects," *Chem. Mater.*, vol. 29, pp. 3793-3799, 2017.
- [7] C. Geng, S. Xu, H. Zhong, A. L. Rogach, and W. Bi, "Aqueous synthesis of methylammonium lead halide perovskite nanocrystals," *Angew. Chem. Int. Ed.*, vol. 57, pp. 9650-9654, 2018.
- [8] Y. Hassan, O. J. Ashton, J. H. Park, G. Li, N. Sakai, B. Wenger, *et al.*, "Facile synthesis of stable and highly luminescent methylammonium lead halide nanocrystals for efficient light emitting devices," *J. Am. Chem. Soc.*, vol. 141, pp. 1269-1279, 2019.